F. Ashmore, *Nature* **365**, 838 (1993).
13. G. D. Housley and J. F. Ashmore, *J. Physiol. (London)* **448**, 73 (1992).
14. J. F. Ashmore and R. W. Meech, *Nature* **322**, 368 (1986); A. H. Gitter and H. P. Zenner, in *Basic Issues in Hearing*, H. Duifhuis, J. W. Horst, H. P. Wit, Eds. (Academic Press, London, 1988), pp. 32–39; J. F. Ashmore, in *Cochlear Mechanisms*, J. P. Wilson and D. T. Kemp, Eds. (Plenum, New York, 1989), pp. 107–113; J. Santos-Sacchi, *J. Neurosci.* **11**, 3096 (1991).
15. J. Santos-Sacchi and D. P. Dilger, *Hearing Res.* **35**, 143 (1988).
16. A. Forge, *Cell Tissue Res.* **265**, 473 (1991).
17. M. Kössl and I. J. Russell, *J. Neurosci.* **12**, 1575 (1992); I. J. Russell and M. Kössl, *Proc. R. Soc. London B* **247**, 97 (1992). The values used here for extracellular responses were confirmed by I. J. Russell as being representative of the most sensitive preparations.
18. P. Dallos, *Hearing Res.* **12**, 89 (1983).
19. P. M. Sellick, R. Patuzzi, B. M. Johnstone, *J. Acoust. Soc. Am.* **72**, 131 (1982).
20. Control of cochlear amplification by extracellular voltages has been mentioned in passing by a number of authors, for example, H. Davis [*Am. J. Otolaryngol.* **2**, 153 (1981)] and (*15*).
21. C. D. Geisler, G. K. Yates, R. B. Patuzzi, B. M. Johnstone, *Hearing Res.* **44**, 241 (1990); M. A. Cheatham and P. Dallos, unpublished data.
22. C. D. Hopkins, *Am. Zool.* **21**, 211 (1981).
23. A. J. Hudspeth and D. P. Corey, *Proc. Natl. Acad. Sci. U.S.A.* **74**, 2407 (1977).
24. Detailed descriptions of the experimental methods have been published (*11*). OHCs were obtained from the cochleas of young anesthetized albino guinea pigs (care and maintenance of animals was in accord with institutional guidelines). For these specific experiments, cells ($n$ = 12) were harvested only from the third and fourth turns of the cochlea; their lengths ranged between 60 and 75 μm and their diameter was uniform (8 to 9 μm). In other experiments, with cells not fully inserted into the microchamber ($n$ = 206), the full range of cell lengths was used. We note that the all-pass nature of the response applies to cells of any length and for any degree of insertion. After removal of segments of the organ of Corti, cells were transferred after enzymatic incubation with Type IV collagenase (0.5 mg/ml; Sigma) to the experimental bath containing either Leibovitz's L-15 medium (Gibco) or Medium 199 (Gibco), supplemented with 15 mM Hepes and 5 mM bovine serum albumin (Sigma) and adjusted to 300 mosM (pH 7.35). Microchambers that held the cells were fabricated from borosilicate glass and had aperture diameters similar to those of OHCs. Cells were drawn into siliconized microchambers by gentle suction. Inserted cells were inspected at high magnification and discarded if there was any sign of induced trauma. All experiments were conducted at room temperature. Electrical command signals were generated from the low-impedance output of a waveform generator board in an IBM 486 clone and were delivered between the electrolytes surrounding and filling the microchamber. Making the fluid within the microchamber positive hyperpolarized the included membrane segment and depolarized the excluded membrane (*11*). Although the microchamber method did not permit us to measure it directly, the asymmetry of the electromotile response is indicative of the cell's resting potential. Cells that are likely to have relatively high resting potentials produce larger shortening than extension-directed responses. Conversely, depolarized cells generate either a symmetrical electromotile response or one with extension dominance (*11*) [J. Santos-Sacchi, *J. Neurosci.* **9**, 2954 (1989)]. All cells in this study had pronounced contraction-directed response asymmetry and, by inference, high membrane potential. Pseudorandom noise is often used to identify the linear filter portion of a nonlinear physiological system [A. R. Møller, *Scand. J. Rehab. Med. Suppl.* **3**, 37 (1974); P. A. Marmarelis and V. Z. Marmarelis, *Analysis of Physiological Systems* (Plenum, New York, 1978)]. We used this signal in order to reduce data collection time. For our parameters, the 3-dB down point of the input was at 19,924 Hz. There are 161 spectral components within this bandwidth, and the voltage applied across the entire cell per spectral line was approximately ±0.6 mV. The extensive data obtained with ternary noise was confirmed in several cells by use of sinusoidal stimuli. The noise floor for the measurement shown in Fig. 2 was between 0.1 and 0.2 nm; thus, noise was clearly not a determinant of the high-frequency asymptote. The cell was imaged through a slit on a photodiode. Cell contraction and expansion modulated the light flux and the photocurrent. The entire stimulus-delivery and measuring apparatus was calibrated by use of the ternary signal input to illuminate the photodiode with a wide-band light-emitting diode and by measurement of its output. The resulting frequency response (corner frequency 18 kHz) of the entire system was used to correct all experimental data. System gain was calibrated for each experimental run by controlled displacement of the image of the cell in the slit.
25. We thank our colleagues M. A. Cheatham, B. Clark, S. Echteler, G. Emadi, D. Z. Z. He, M. Ruggero, J. Siegel, I. Sziklai, and S. Vranic-Sowers for their contributions and their comments on the manuscript. Supported by NIH and the American Hearing Research Foundation.

7 September 1994; accepted 27 December 1994

# TECHNICAL COMMENTS

## Models of $Ca^{2+}$ Release Channel Adaptation

Channel adaptation (*1*) involves complex behavior of the sarcoplasmic reticulum (SR) $Ca^{2+}$ release channel (ryanodine receptor, RyR). The adaptive behavior is different from conventional ion channel behavior in that adapting channels transiently activate (open) in response to repeated increments of agonist ($Ca^{2+}$). No published kinetic model known to us could adequately account for this adaptation. We propose a model that readily accounts for the complexities associated with adaptation.

The model is based on the established tetrameric RyR channel structure. Biochemical studies indicate that at least three high affinity $Ca^{2+}$-binding sites exist per monomer (*2*). We postulate that one kind of binding site (the O-domain) tends to open the channel when activated by $Ca^{2+}$ and another (the A-domain) tends to close (adapt) it. Thus, the tetramer would then have four O-domains and four A-domains. The model uses the following rules to describe the behavior of the channel. The channel opens when the number of occupied O-domains (O) on the tetramer exceeds or equals the number of active A-domains (A), that is, $O \geq A$. However when $A > O$, or $O$ = zero, the channel remains closed. In order for the model to fit the published experimental data, each O-domain must be cooperative ($n$ = 2) and have lower affinity and faster $Ca^{2+}$-binding kinetics than each A-domain (Fig. 1, methods). At high [$Ca^{2+}$], when both O- and A-domains are occupied, the data are best fit if the channel opens 75% of the time when O = A.

This model predicts that the steady-state probability of a channel being open ($P_o$) varies as a monotonic increasing function of [$Ca^{2+}$] (Fig. 1A) and that fast $Ca^{2+}$ steps trigger transient bursts of channel activity well above the steady-state level (Fig. 1, A and B). The predicted concentration- and time-dependent occupancy of O- and A-domains on a tetramer during two step increases in [$Ca^{2+}$] are shown (Fig. 1C). Our model accurately accounts for the experimental data which defines RyR adaptation (*1*). Published models (*3*) cannot reproduce the observed second transient response of the "apparently inactivated" channel. This is expected in light of theoretical thermodynamic analysis of RyR behavior, which indicates that one would need a large number of $Ca^{2+}$-binding sites to explain adaptation (*4*).

Our adaptation model resolves apparently contradictory results and suggests future areas of experimentation. The model explains how elevated [$Ca^{2+}$] can both apparently "inactivate" peak SR $Ca^{2+}$ release in situ and increases steady-state $P_o$ of individual RyR channels. It also enables the SR $Ca^{2+}$ release channels to respond to $d[Ca^{2+}]/dt$, a classical observation of Fabiato (*3*) in skinned muscle. Adaptation in vitro, however, appears too slow to regulate SR $Ca^{2+}$ release in cells (*1*, *5*). Thus, the model predicts that (as yet) unknown endogenous factors may accelerate the rate of adaptation (for example, modulate binding kinetics of A-domain) in cells. Finally, this model may apply to other intracellular $Ca^{2+}$ release channels as it could also provide the basis for the incremental, or "quantal," $Ca^{2+}$ release from inositol triphosphate ($IP_3$)–sensitive $Ca^{2+}$ stores (*6*). [An $IP_3$ receptor channel tetramer with O- and A-domains incrementally occupied by $IP_3$ may explain the quantal character of the $IP_3$-induced channel opening as well as the incremental channel "inactivation" observed by Hajnoczky and Thomas (*6*)].

Thus, we propose that the complex adaptive channel behavior arises from the assembly of simple interactive monomers. Although each monomer by itself is not able to produce the complex behavior, the interplay among the monomers exponentially extends the functional flexibility of the assembled unit.

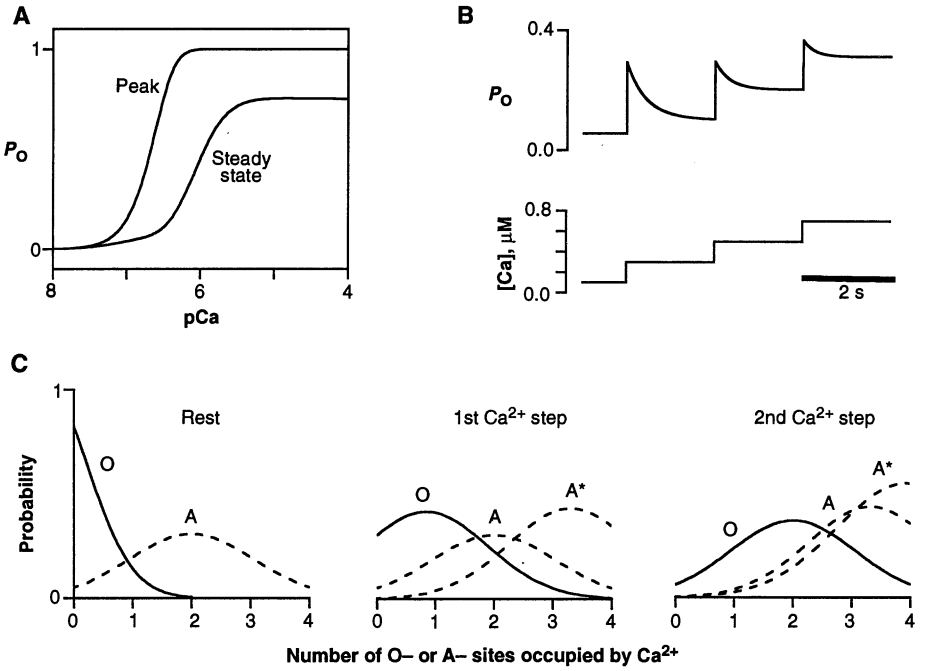


**Fig. 1.** Modeling ryanodine receptor adaptation. (**A**) Transient and steady-state $Ca^{2+}$-dependence of the model channel activity. Peak $P_o$ is obtained during a $[Ca^{2+}]$ step from zero to the designated $[Ca^{2+}]$. (**B**) Repeated activation of the model channel by incremental $[Ca^{2+}]$ steps. The kinetics of channel adaptation are only slightly affected by the concentration of $[Ca^{2+}]$. (**C**) Concentration- and time-dependent binding of $Ca^{2+}$ to the O-domains (solid lines) and A-domains (dash lines) within a channel tetramer. At 100 nM resting $[Ca^{2+}]$, most of the O-domains are empty (O-curve) while the A-domains are half-filled (A-curve), leading to a low $P_o$ at rest. Upon a step increase of $[Ca^{2+}]$, more O-domains are bound with $Ca^{2+}$, as indicated by the rightward shift of the O-curve. Adaptation occurs as the A-curve (at the time of $[Ca^{2+}]$ change) becomes the A*-curve (two seconds later). In response to the second $[Ca^{2+}]$ step, the O-curve is immediately shifted further to the right and this underlies the genesis of the second peak in $P_o$. Equilibration of the A-domains with the new $[Ca^{2+}]$ level accounts for the second decline in $P_o$ as curve A becomes A*. The dissociation constants ($K_d$) for $Ca^{2+}$ binding to O- and A-domains are taken as 0.5 μM and 0.1 μM, respectively. Hill coefficients are 2 and 1 for O-domains and A-domains, respectively. $Ca^{2+}$ binding to O-domains is assumed to be diffusion-limited. $Ca^{2+}$ binding to the A-domains occurs with an on-rate of $5 \times 10^6\ M^{-1}\ S^{-1}$ and off-rate of $0.5\ S^{-1}$. Solutions of the model were obtained analytically.


***Heping Cheng***
*Department of Physiology, School of Medicine, University of Maryland, Baltimore, MD 21201, USA*
***Michael Fill***
*Department of Physiology, University of Texas Medical Branch, Galveston, TX 77555, USA*
***Hector Valdivia***
*Department of Physiology, Medical School, University of Wisconsin, Madison, WI 53706, USA*
***W. J. Lederer***
*Department of Physiology and Medical Biotechnology Center, School of Medicine, University of Maryland, Baltimore, MD 21201, USA*


## REFERENCES AND NOTES


1. S. Györke and M. Fill, *Science* **260**, 807 (1993).
2. S. R. W. Chen, L. Zhang, D. H. MacLennan, *J. Biol. Chem.* **267**, 23318 (1992).
3. A. Fabiato, *J. Gen. Physiol.* **85**, 247 (1985); *ibid.*, p. 189; *ibid.*, p. 291.
4. M. D. Stern, personal communication.
5. K. R. Sipido and W. G. Wier, *J. Physiol. (London)* **435**, 605 (1991); M. B. Cannell, H. Cheng, W. J. Lederer, *Biophysical J.* **67**, 1942 (1994).
6. M. J. Berridge, *Nature* **361**, 315 (1993); G. Hajnoczky and A. P. Thomas, *ibid.* **370**, 474 (1994).


7. This work was supported by NIH, American Heart Association, the Medical Biotechnology Center, and University of Maryland at Baltimore DRIF awards.

13 September 1994; accepted 12 December 1994


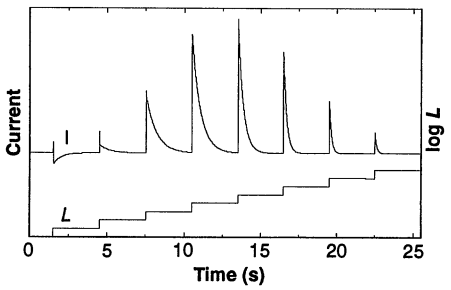


**Fig. 1.** Numerical simulation of exact adaptation with successive stimuli. Upper trace shows current, lower trace shows ligand concentration. Steps are 3 s in duration. $L = 0$ from 0 to 1.5 s, and it then increases in exponential steps, that is, 0.0316, 0.1, 0.316, 1, . . . 100 mM. Rate constants are $k_1 = 1\ s^{-1}$, $k_{-1} = 100\ s^{-1}$, $k_2 = 10\ s^{-1}$, $k_{-2} = 0.1\ s^{-1}$, $k_r = 1000\ mM^{-1}\ s^{-1}$, $k_{-r} = 12000\ s^{-1}$, $k_d = 2000\ mM^{-1}\ s^{-1}$, $k_{-d} = 2.4\ s^{-1}$. Spectral expansion of the transition matrix was used in this simulation.

The ryanodine receptor channel in bilayers displays unusual kinetics (*1*). When Ca is elevated, the channels open and then appear to inactivate. However, in contrast to traditional inactivation such as observed in the acetylcholine receptor, when Ca is further increased the channels reopen and again appear to inactivate. Thus the channel acts as a differentiator, responding primarily to changes in concentration. To avoid confusion with the term inactivation, this reactivatable kind of behavior is termed adaptation.

In adaptive behavior, there is a peak in the response associated with every increase in ligand concentration, and the steady-state response may be independent of the ligand concentration (Fig. 1). Adaptive behavior has been analyzed in the context of bacterial chemoreception (*2*, *3*), and the results are readily transferred to channels. The reaction can be described by a simple Markov scheme in thermal equilibrium.

Following the notation of Segel *et al.* (*3*), we consider the reaction (Fig. 2) where $L$ represents the ligand, states X and D are open, states R and Y are shut, and the rate constants are as indicated. Segel *et al.* (*3*) assume for simplicity that the binding reactions, R↔X and D↔Y are fast compared to the allosteric reactions, R↔D and X↔Y. However, the characteristic adaptive behavior is not dependent upon this assumption.

There are three main conditions to be satisfied by parameters of the model, (i) that the system adapts, (ii) that the peak activity in response to a step input be significantly greater than the steady-state activity, and (iii) that the system be in thermal equilibrium, that is, satisfy detailed balance. In the most extreme case, called exact adaptation (Fig. 1), the steady-state activity is independent of ligand concentration. We have made the additional assumption that the channel has only two conductances, open and closed. One can show that,

1) If the channel is mostly closed in the absence of ligand, then R and Y must be shut and D and X open.

2) For exact adaption, $K_1 \cdot K_2 = 1$, where $K_1 = k_{-1}/k_1$ and $K_2 = k_{-2}/k_2$. For weaker adaptation, that is where the steady-state activity increases with ligand concentration, $K_1 K_2 > 1$, and where it decreases with concentration, $K_1 K_2 < 1$.

3) For microscopic reversibility, $K_1 K_D = K_2 K_R$ where $K_R = k_{-r}/k_r$ and $K_D = k_{-d}/k_d$.

4) The peak current following a step

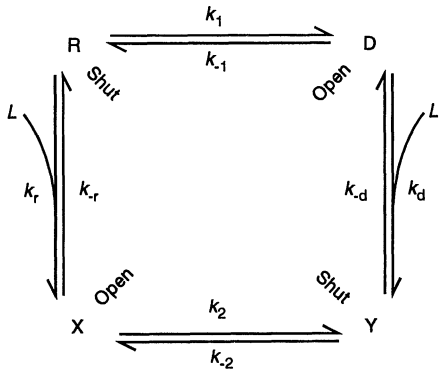


**Fig. 2.** Reaction scheme of an adapting channel. *L* represents the ligand to be bound, states X and D are open, and states R and Y are shut.

change in $L$ is a function of concentration and the rate constants. In general, if the channels are mostly closed in the absence of ligand, the peak transient current will be significant. In the limiting case of a step from $L = 0$ to $L = \infty$, the gain which is defined as the ratio of peak to steady-state current, is given by $G = K_1 - 1$.

An intuitive understanding of adaptive behavior is perhaps best gained by examining the extremes. When $L = 0$, the channel exists only in states R and D. If $K_1 \gg 1$, the probability of being open, $P_o$, is small. When $L = \infty$, the channel exists only in states X and Y and $P_o$ is the same as before since $K_2 = 1/K_1$. Thus, in steady-state $P_o$ is independent of ligand concentration.

For the transient case consider a step from $L = 0$ to $\infty$. When $L = 0$, the channel is mostly in state R. As L is jumped to $\infty$, the probability of being in X, which is an open state, approaches 1. With time, X (and D) drain into Y, which is closed, and the system attains the equilibrium value of $P_o$. The system saturates when R is depleted since addition of ligand cannot produce any further transitions to X.

The simulation (Fig. 1) created with the use of the full kinetics and without an assumption of equilibrium of the binding reactions yields a transient response that has several phases, which are most easily seen at the lowest concentrations. Following a step increase in $L$ there is a rapid increase in current as channels are shifted from R to X. This is followed by a rapid drop in current with time constant, $\tau = 1/(k_{-r} + k_r)$, as the reaction R↔X reaches equilibrium. In the next phase, depending upon the value of $L$, the current may be higher or lower than the basal level (compare the first and second concentration steps of Fig. 1). For the exactly adapting case (and for certain other combinations of rate constants) there is always a drop in the resting current at sufficiently low concentrations of $L$. It is difficult to gain an intuitive understanding of this biphasic process because the result depends on the values of the rate constants. However, in a handwaving sense, the decrease arises because during the rapid increase in X, some of X (open) is carried to Y (closed) before the R↔X equilibration is complete. There are then fewer channels in the pool X + R, and the equilibrium constant $K_r$, which strongly favors R at low concentrations, causes X to fall below the steady-state value.

The model (Fig. 2) can explain much of the data presented by Györke and Fill (*1*) and makes predictions about kinetics not yet reported. It explains the adaptive behavior, the difference in $K_d$ between the peak and steady-state responses (provided $K_1K_2 > 1$). It predicts (simulations not shown) the modal gating behavior seen in their single-channel data [figure 3 of (*1*)]. It also predicts that (for the simple scheme of Fig. 2) the open and closed time distributions will both have two components, and that only one of each will be ligand dependent. For example, the open state lifetimes will be $\tau_X = 1/(k_{-r} + k_{-2})$ and $\tau_D = 1/(k_{-1} + k_dL)$. Finally, it suggests that for sufficiently low concentrations of $Ca^{2+}$ there may be a drop in $P_o$ rather than an increase.

The response time for adaptation is dependent upon the concentration of $L$ [equations 50 and 51 of (*3*)]. In the limiting cases of $L \rightarrow 0$ and $L \rightarrow \infty$, the time constants are $1/(k_1 + k_{-1})$ and $1/(k_2 + k_{-2})$, respectively. Yasui *et al.* (*4*) have shown that adaptation of ryanodine receptors in myocytes is about 100-fold faster than in bilayers (*1*). If the model's kinetics (Fig. 2) apply, then we have to assume that the R↔D and X↔Y transition rates are modified during reconstitution.

The model is rich in potential behaviors, aside from being adaptive. For example, the slow response amplitude can be a biphasic function of concentration (Fig. 1). Depending on the constants, the model can also show a maximum (or minimum) in the steady state current so that a titration could show apparent saturation followed by unsaturation. If $L$ were an inhibitor, the system could show inhibition at high concentrations and activation at low concentrations.

The model can be changed without altering its adaptive behavior. As pointed out by Segel *et al.* (*3*), it can be reduced to three states, but in the case of a channel, this can only be satisfied with a channel that has zero probability of being open in the absence of ligand. Toward increasing complexity, the open states could be made into rapidly converting compound states so that the mean conductances would lie between open and closed. If the binding kinetics were not made infinitely fast, adaptation would persist, but the peak responses would be rounded.

Adaptive behavior may apply to other systems beside the ryanodine receptor, notably the inositol trisphosphate ($IP_3$) receptor, which appears to display similar behavior (*5*). A variety of explanations have been offered to account for its adaptation including populations of receptors with different affinities (*5*), but adaptive kinetics may be a more economical explanation. As required by the adaptive model, $IP_3$ has recently been shown to be capable of closing $IP_3$ channels (*6*). The fact that both $Ca^{2+}$ and $IP_3$ can activate (*7*) and inhibit the channel requires adding states to the model, unless the R↔D and X↔Y transitions are made $Ca^{2+}$-dependent. The adaptive behavior of $Ca^{2+}$ release channels may account for the termination of $Ca^{2+}$ waves (*8*).

One may imagine applications of adaptive kinetics to other sensory systems such as hair cells of the cochlear-vestibular systems (*9*, *10*). In this case, the system would be driven by force instead of ligand binding. To account for the mechanical sensitivity of gating, the gating elements of the channel in states X and Y would be physically larger than those in states R and D (*11*). Adaptation would then reflect only properties of the channel gating process rather than auxiliary elements (*12*). Despite the appeal of adaptive kinetics at the molecular level, it is important to bear in mind that adaptive behavior does not imply a particular mechanism.

***F. Sachs***
***F. Qin***
*Department of Biophysics,*
*State University of New York,*
*Buffalo, NY 14214, USA*
***P. Palade***
*Department of Physiology and Biophysics,*
*Medical Branch,*
*University of Texas,*
*Galveston, TX 77555, USA*

## REFERENCES

1. S. Györke and M. Fill, *Science* **260**, 807 (1993).
2. B. E. Knox, P. N. Devreotes, A. Goldbeter, L. A. Segel, *Proc. Natl. Acad. Sci. U.S.A.* **83**, 2345 (1986).
3. L. A. Segel, A. Goldbeter, P. N. Devreotes, B. E. Knox, *J. Theor. Biol.* **120**, 151 (1986).
4. K. Yasui, P. Palade, S. Györke, *Biophy. J.* **67**, 457 (1994).
5. L. Missiaen, J. B. Parys, H. De Smedt, M. Oike, R. Casteels, *Mol. Cell. Endocrin.* **98**, 147 (1994).
6. G. Hajnoczky and A. P. Thomas, *Nature* **370**, 474 (1994).
7. L. Combettes, P. Champeil, E. A. Finch, S. M. Goldin, *Science* **265**, 813 (1994).
8. A. Atri, Amundson, D. Clapham, J. Sneyd, *Biophys. J.* **65**, 1727 (1993).
9. J. A. Assad and D. P. Corey, *J. Neurosci.* **12**, 3291 (1992).
10. J. O. Pickles and D. P. Corey, *Trends Neurosci.* **15**, 254 (1992).
11. J. Howard and A. J. Hudspeth, *Neuron* **1**, 189 (1988).
12. P. G. Gillespie and A. J. Hudspeth, *Proc. Natl. Acad. Sci. U.S.A.* **90**, 2710 (1993).

28 September 1994; accepted 12 December 1994